Poly(phenylenevinylene)-Attached Phenoxyl Radicals: Ferromagnetic Interaction through Planarized and π-Conjugated Skeletons

Hiroyuki Nishide,*,† Takashi Kaneko,†,§ Takeshi Nii,† Kohya Katoh,† Eishun Tsuchida,*,† and Paul M. Lahti‡

Contribution from the Department of Polymer Chemistry, Waseda University, Tokyo 169, Japan, and Department of Chemistry, University of Massachusetts, Amherst, Massachusetts 01003

Received May 20, 1996[⊗]

Abstract: Chemically stable poly[2-(3,5-di-*tert*-butyl-4-oxyphenyl)-1,4(*p*)-phenylenevinylene], poly[4-(3,5-di-*tert*-butyl-4-oxyphenyl)-1,3(*m*)-phenylenevinylene], and poly[4-(3,5-di-*tert*-butyl-4-oxyphenyl)-1,2(*o*)-phenylenevinylene] were synthesized *via* the polymerization of 4-bromo-2-(3,5-di-*tert*-butyl-4-acetoxyphenyl)styrene, 5-bromo-2-(3,5-di-*tert*-butyl-4-acetoxyphenyl)styrene, and 2-bromo-4-(3,5-di-*tert*-butyl-4-acetoxyphenyl)styrene, respectively, using a palladium catalyst. The *o*- and *p*-polyradicals, even with their spin concentration of 0.6 spin/unit, displayed *S* values of 4/2 to 5/2 ($S = 5/2$ for the *o*-polyradical with a degree of polymerization of 17 and a spin concentration of 0.68), while the *m*-polyradical has a singlet ground state. A long-range intramolecular through-bond ferromagnetic exchange interaction was realized between the pendant unpaired electrons for the *o*- and *p*-polyradicals, in accordance with theoretical predictions based on the molecular connectivity. The average value of the exchange coupling constant for the *o*-polyradical, $2\bar{J} = 48 \pm 6$ cm^{-1}, was larger than $2\bar{J} = 32 \pm 2$ cm^{-1} for the *p*-polyradical, while they were almost coincident with or much larger than the exchange coupling constants for the corresponding diradical model compounds. Both force field calculations and spectroscopic results indicated a less hindered steric structure with a planarized π-conjugated skeleton for the *o*-polyradical.

Introduction

Much effort has been expended in synthesizing purely organic polyradicals which are expected to display molecular-based magnetism.[1−4] For a π-conjugated and alternant but non-Kekulé-type organic molecule bearing plural radical centers, formulations based on MO or VB theory are effective for predicting the spin multiplicity or spin quantum number (*S*) at the ground state (GS), which is clearly related to the molecular connectivity or substitution positions of the radical centers at the conjugated coupler.[5] Longuet-Higgins[5a] showed by applying Hückel theory to alternant molecules with *N* π-centers and *T* double bonds in the structure of highest Kekulé bondedness that the number of nonbonding molecular orbitals (NBMOs) is given by eq 1. A molecule with multiple NBMOs is expected to

$$\text{no. of NBMOs} = N - 2T \tag{1}$$

possess a multiplet GS if one assumes an extension of Hund's rule to molecules. This number of NBMOs is thus equal to the number of unpaired electrons to a first approximation for many alternant molecules.

Table 1. Expected Spin State for Stilbene Diradicals and Poly(phenylenevinylene)-Attached Polyradicals

compound	no. of NBMOs	$S = \lvert n^* - n^\circ \rvert/2$	connectivity for NBMO
o,*o*′-, *o*,*p*′-, and *p*,*p*′-**1**	0	0	
m,*m*′-**1**	2	0	doubly disjoint
o,*m*′- and *m*,*p*′-**1**	2	1	nondisjoint
m-**2** (*o*,*p*′) and *o*,*o*′- and *p*,*p*′-**2** isomers	0	0	
m,*m*′-**2** isomers	2*n*	0	doubly disjoint
o-**2** (*m*,*p*′) and *p*-**2** (*o*,*m*′)	2*n*	*n*	nondisjoint

According to Ovchinnikov's formulation[5e] based on VB theory, GS *S* is predicted by half the difference between the numbers of starred and unstarred π-centers, as given in eq 2.

$$S = |n^* - n^\circ|/2 \tag{2}$$

Simple enumeration of the molecular connectivity thus leads to the finding of GS *S*. Borden and Davidson[5c] have noted that a decreased exchange interaction between unpaired electrons in a diradical will minimize the triplet−singlet energy gap (ΔE_{T-S}) if the two NBMOs are confineable to separate regions of the molecule. Such a system is called a disjoint. On the contrary, a triplet GS with a large magnitude of ΔE_{T-S} is expected for a nondisjoint molecule, whose NBMOs cannot be localized in different regions. By applying these models to the stilbene diradicals **1**, the electronic GSs of **1** are as shown in

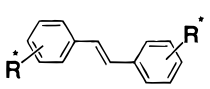

1

Table 1. A high-spin ($S = 2/2$) GS is expected for the *o*,*m*′- and *m*,*p*′-isomers and a low-spin ($S = 0$) GS for all the other

† Waseda University.
‡ University of Massachusetts.
§ Present address: Graduate School of Science and Technology, Niigata University, Niigata 950-21, Japan.
⊗ Abstract published in *Advance ACS Abstracts,* September 15, 1996.

(1) (a) Miller, J. S. *Adv. Mater*. **1990**, *2*, 98. (b) Miller, J. S.; Epstein, A. J. *Angew. Chem., Int. Ed. Engl*. **1994**, *33*, 385.
(2) Dougherty, D. A. *Acc. Chem. Res.* **1991**, *24*, 88.
(3) Iwamura, H.; Koga, N. *Acc. Chem. Res.* **1993**, *26*, 346.
(4) Rajca, A. *Chem. Rev.* **1994**, *94*, 871.
(5) (a) Longuet-Higgins, H. C. *J. Chem. Phys.* **1950**, *18*, 265. (b) Mataga, N. *Theor. Chim. Acta* **1968**, *10*, 372. (c) Borden, W. T.; Davidson, E. R. *J. Am. Chem. Soc.* **1977**, *99*, 4587. (d) Itoh, K. *Pure Appl. Chem.* **1978**, *50*, 1251. (e) Ovchinnikov, A. A. *Theor. Chim. Acta* **1978**, *47*, 297. (f) Klein, D. J.; Nelin, C. J.; Alexander, S.; Masten, F. A. *J. Chem. Phys.* **1982**, *77*, 3101.

S0002-7863(96)01721-0 CCC: $12.00

Chart 1

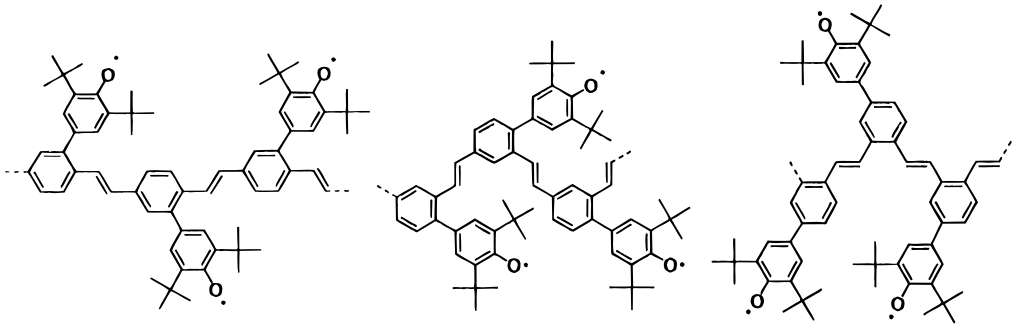

p-**2** *m*-**2** *o*-**2**

isomers such as *m,m′*. For example, our computational and experimental studies of the stilbene dinitroxide isomers have supported these qualitative expectations.[6]

The models for diradical molecules with high-spin GS have been extended to organic π-conjugated polyradicals. Major synthetic approaches have been based on cross-conjugated polyradicals or on radicals formed in main chains to satisfy the radical connectivity. Typical examples are the polyradicals derived from poly(1,3-phenylenemethylene)[7] and 1,3-connected linear[8] and dendritic polyphenylmethanes[9] which have GS $S = 5/2 \times 2$ (carbene-based), 4/2, and 10/2, respectively. Although these displayed strong through-bond ferromagnetic coupling between two unpaired electrons in the 1,3-phenylene-connected radicals at low temperature, even a small number of defects in the polyradicals significantly prevented an increase in the resulting *S* due to their radical formation through the cross-conjugated structures. Besides this drawback, these polyradicals, except for a few molecules,[10] lacked chemical stability at room temperature.

Another synthetic approach focuses on π-conjugated linear polymers bearing pendant or side-chain radical groups, which are attached to a π-conjugated polymer skeleton and have substantial chemical stability. Intramacromolecular and through-bond interactions between pendant spins have often been theoretically studied for this type of polyradical, mainly on polyacetylene-based radicals.[5e,f] We have synthesized poly(phenylacetylene)s bearing various types of side radical groups such as di-*tert*-butylphenoxyl, galvinoxyl, and *tert*-butyl nitroxide.[11] However, the expected ferromagnetic interactions could not be observed to date for any poly(phenylacetylene)-attached radicals,[11,12] including the reports by other groups.[13] We concluded that coplanarity both in the poly(phenylacetylene) skeleton itself and in the dihedral angle with a pendant radical is essential to realize a through-bond exchange interaction leading to intramolecular ferromagnetic behavior.[12]

Poly(phenylenevinylene) is a possible candidate for an effective skeleton for π-conjugated polyradicals, because of its developed conjugation, coplanarity, and solvent solubility after substitution on the phenylene ring.[14] The theoretical predicted spin states in Table 1 and experimental study of model diradicals connected with stilbene couplers[6,15] suggest that poly(1,4(*p*)- and 1,2(*o*)-phenylenevinylene)s bearing π-conjugated and built-in radical groups on every monomer unit (**2** in Chart 1) will show intramacromolecular ferromagnetic coupling to become a GS high-spin polymer. The molecular connectivity in all the *p*- and *o*-**2** systems leads to the expectation that their spin quantum numbers at low temperature will, ideally, be proportional to the degree of polymerization. Recently, we have succeeded in designing an intramacromolecular ferromagnetic exchange between pendant unpaired electrons, by synthesizing poly(1,4- and 1,2-phenylenevinylene)s that are 2- or 4-substituted with the 3,5-di-*tert*-butyl-4-oxyphenyl[16] or *N*-*tert*-butyl-*N*-oxyamino group.[17] This paper describes intramacromolecular ferromagnetic spin alignment induced by synthesizing poly(phenylenevinylene)s bearing pendant phenoxyl radicals with restricted head-to-tail linkage and substituent connectivity. We show that the prediction of high- and low-spin ground states is confirmed by ESR and SQUID measurements for different connectivities in the polymer. Finally, the ferromagnetic interaction through the planarized and π-conjugated poly(phenylenevinylene) skeleton is discussed in comparison to analogous results for the corresponding diradical compounds, by using semiempirical calculations and spectroscopic results.

Results and Discussion

Polymer Synthesis and Characterization. 4-Bromo(or iodo)-2-(3,5-di-*tert*-butyl-4-acetoxyphenyl)styrene (*p*-**3″** (or *p*-**3I″**)), 4-bromo-2-(3,5-di-*tert*-butyl-4-hydroxyphenyl)styrene (*p*-**3′**), 5-bromo-2-(3,5-di-*tert*-butyl-4-acetoxyphenyl)styrene (*m*-**3″**), and 2-bromo-4-(3,5-di-*tert*-butyl-4-acetoxyphenyl)styrene (*o*-**3″**) were synthesized as monomers to be linked with head-

(6) Yoshioka, N.; Lahti, P. M.; Kaneko, T.; Kuzumaki, Y.; Tsuchida, E.; Nishide, H. *J. Org. Chem.* **1994**, *59*, 4272.

(7) Fujita, I.; Teki, Y.; Takui, T.; Kinoshita, T.; Itoh, K.; Miko, F.; Sawaki, Y.; Iwamura, H.; Izuoka, A.; Sugawara, T. *J. Am. Chem. Soc.* **1990**, *112*, 4074.

(8) Utamapanya, S.; Kakegawa, H.; Bryant, L.; Rajca, A. *Chem. Mater.* **1993**, *5*, 1053.

(9) (a) Rajca, A.; Utamapanya, S.; Thayumanavan, S. *J. Am. Chem. Soc.* **1992**, *114*, 1884. (b) Rajca, A.; Utamapanya, S. *J. Am. Chem. Soc.* **1993**, *115*, 10688.

(10) (a) Ishida, T.; Iwamura, H. *J. Am. Chem. Soc.* **1991**, *113*, 4238. (b) Kanno, F.; Inoue, K.; Koga, N.; Iwamura, H. *J. Am. Chem. Soc.*, **1993**, *115*, 13267. (c) Veciana, J.; Rovira, C.; Ventosa, N.; Crespo, M. I.; Palacio, F. *J. Am. Chem. Soc.* **1993**, *115*, 57.

(11) (a) Nishide, H.; Yoshioka, N.; Inagaki, K.; Tsuchida, E. *Macromolecules* **1988**, *21*, 3119. (b) Nishide, H.; Yoshioka, N.; Kaneko, T.; Tsuchida, E. *Macromolecules* **1990**, *23*, 4487. (c) Nishide, H.; Yoshioka, N.; Inagaki, K.; Kaku, T.; Tsuchida, E. *Macromolecules* **1992**, *25*, 569. (d) Yoshioka, N.; Nishide, H.; Kaneko, T.; Yoshiki, H.; Tsuchida, E. *Macromolecules* **1992**, *25*, 3838. (e) Nishide, H.; Kaneko, T.; Yoshioka, N.; Akiyama, H.; Igarashi, M.; Tsuchida, E. *Macromolecules* **1993**, *26*, 4567.

(12) Nishide, H.; Kaneko, T.; Igarashi, M.; Tsuchida, E.; Yoshioka, N.; Lahti, P. M. *Macromolecules* **1994**, *27*, 3082.

(13) (a) Fujii, A.; Ishida, T.; Koga, N.; Iwamura, H. *Macromolecules* **1991**, *24*, 1077. (b) Miura, Y.; Matsumoto, M.; Ushitani, Y.; Teki, Y.; Takui, T.; Itoh, K. *Macromolecules* **1993**, *26*, 6673.

(14) (a) Lahti, P. M.; Ichimura, A. *J. Org. Chem.* **1991**, *56*, 3030. (b) Nishide, H.; Kaneko, T.; Kuzumaki, Y.; Yoshioka, N.; Tsuchida, E. *Mol. Cryst. Liq. Cryst.* **1993**, *232*, 143.

(15) Mitsumori, T.; Koga, N.; Iwamura, H. *J. Phys. Org. Chem.* **1994**, *7*, 43.

(16) Nishide, H.; Kaneko, T.; Nii, T.; Katoh, K.; Tsuchida, E.; Yamaguchi, K. *J. Am. Chem. Soc.* **1995**, *117*, 548.

(17) Kaneko, T.; Toriu, S.; Kuzumaki, Y.; Nishide, H.; Tsuchida, E. *Chem. Lett.* **1994**, 2135.

Scheme 1

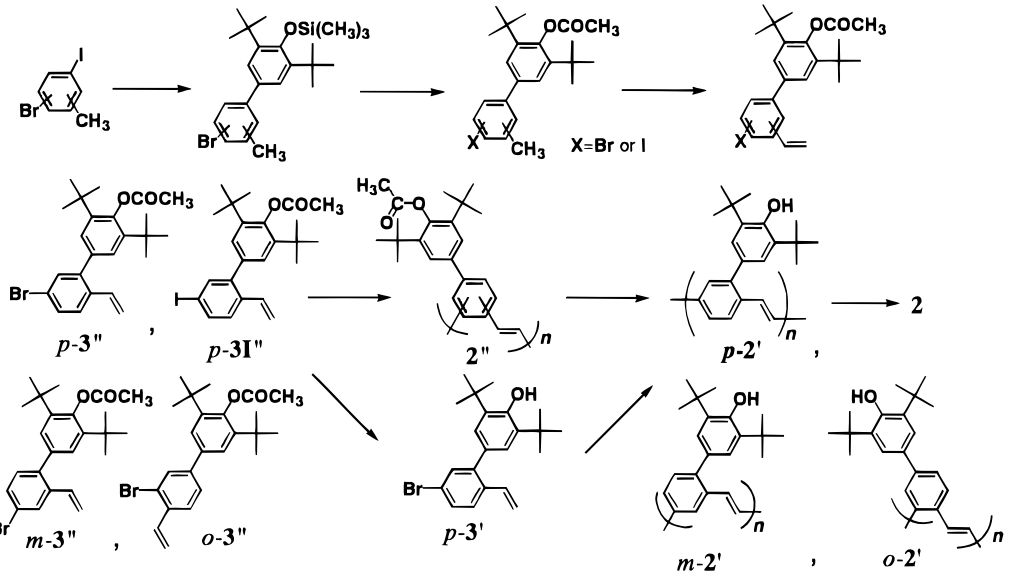

Chart 2

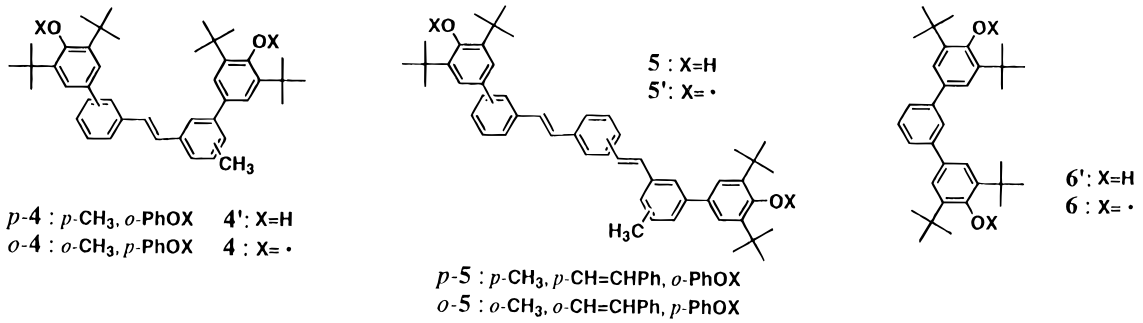

to-tail bonds *via* the arylation of olefins with aryl bromides by the Heck reaction,[18] according to Scheme 1. The 3,5-di-*tert*-butyl-4-acetoxyphenyl group was introduced onto 4-bromo-2-iodotoluene, 5-bromo-2-iodotoluene, and 2-bromo-4-iodotoluene, respectively, by selective coupling at the iodo position with [3,5-di-*tert*-butyl-4-(trimethylsiloxy)phenyl]magnesium bromide using a nickel catalyst.[19a] The trimethylsiloxy group was exchanged for an acetoxy group, and the methyl group was modified to a vinyl group *via* the Wittig reaction[19b] (for details see the Experimental Section). *p*-**3″**, **3I″**, **3′**, *m*-**3″**, and *o*-**3″** were polymerized using a catalyst of palladium acetate and tri-*o*-tolylphosphine to yield the polymers *p*-**2″**, *m*-**2″**, and *o*-**2″**, respectively (see Table 3 in the Experimental Section). The polymerization of *p*-**3″** proceeded more effectively than that of *p*-**3′**, suggesting a poisoning effect of the hydroxyl group against the palladium catalyst. While the iodostyrene *p*-**3I″** was polymerizable at lower temperature in comparison with the bromostyrene *p*-**3″**, the molecular weight of the final polymers depended on their solubility in the polymerization solvent (DMF in this case). A similar polymerization profile was observed for *m*- and *o*-**3″**.

The polymers *p*-, *m*-, and *o*-**2″** were obtained as yellow powders that were soluble in common solvents such as $CHCl_3$, benzene, THF, and acetone. The degree of polymerization (DP) measured by GPC agreed well with the terminal bromine content determined from elemental analysis, *e.g.*, for *p*-**2″** with DP = 31 by GPC and DP = 28 by bromine analysis, which supports a linear polymer structure. Head-to-tail and *trans*-vinylene linkage structures of the polymers were confirmed by ^{13}C-NMR (12 carbon absorption peaks ascribed to the phenylene rings and vinylene), the IR absorptions, and the fluoresence attributed to a *trans*-stilbene moiety (for details see the Experimental Section). The restricted primary structure, which is essential for the following magnetic study, was established through the polymerization *via* the Heck reaction of the phenylene monomer possessing vinyl and bromo (or iodo) functional groups. The polymers *p*-, *m*-, and *o*-**2″** were converted to the corresponding hydroxypolymers *p*-, *m*-, and *o*-**2′**, respectively, after complete elimination of the protection acetyl group.

4-Methyl-3,2′-bis(3,5-di-*tert*-butyl-4-oxyphenyl)stilbene (*p*-**4**), 2-methyl-5,4′-bis(3,5-di-*tert*-butyl-4-oxyphenyl)stilbene (*o*-**4**), 1-[4-methyl-3-(3,5-di-*tert*-butyl-4-oxyphenyl)styryl]-4-[2-(3,5-di-*tert*-butyl-4-oxyphenyl)styryl]benzene (*p*-**5**), 1-[2-methyl-5-(3,5-di-*tert*-butyl-4-oxyphenyl)styryl]-2-[4-(3,5-di-*tert*-butyl-4-oxyphenyl)styryl]benzene (*o*-**5**), and *m*-bis(3,5-di-*tert*-butyl-4-oxyphenyl)benzene (**6**), represented in Chart 2, were synthesized as diradical analogs to investigate the electronic state and spin exchange interaction in **2.** For example, the UV−vis absorption maximum (λ_{max}) and ionization threshold (I^{th}) estimated by photoelectron spectroscopy[20] were 312 nm and 5.7 eV for *p*-**4′** and 364 nm and 5.9 eV for *p*-**5′**, respectively. For the corresponding polymer *p*-**2′**, λ_{max} = 386 nm and I^{th} = 5.6 eV. This comparison and the previously reported λ_{max} data of poly(phenylenevinylene)s[21] indicate a developed π-conjugation in

(18) (a) Heck, R. F. *Org. React.* **1982**, *27*, 345. (b) Greiner, A.; Heitz, W. *Makromol. Chem. Rapid Commun.* **1988**, *9*, 581.

(19) (a) Tamao, K.; Sumitani, K.; Kiso, Y.; Zembayashi, M.; Fujioka, A.; Kodama, S.-i.; Nakajima, I.; Minato, A.; Kumada, M. *Bull. Chem. Soc. Jpn.* **1976**, *49*, 1958. (b) Märkl, G.; Merz, A. *Synthesis* **1973**, 295.

(20) Kaneko, T.; Ito, E.; Seki, K.; Tsuchida, E.; Nishide, H. *Polym. J.* **1996**, *28*, 182.

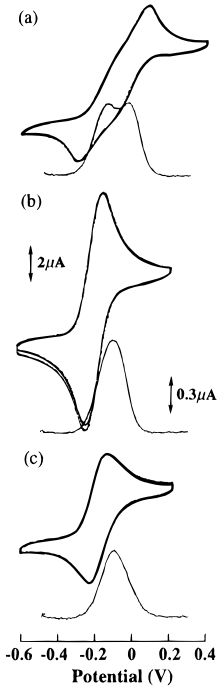

Figure 1. Cyclic voltammograms and differential pulse voltammograms for the di- and polyphenolate anions **6′** (a), *o*-**4′** (b), and *o*-**2′** (c), in dichloromethane with tetrabutylammonium tetrafluoroborate and tetramethylammonium hydroxide.

Scheme 2

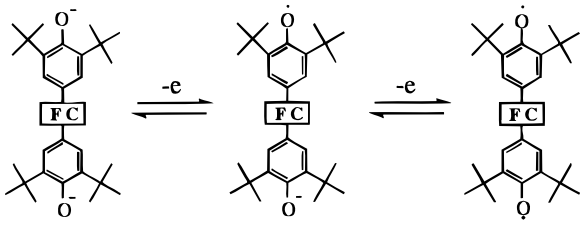

the skeleton of *p*-**2′** and an extension of the π-conjugation with the DP of poly(phenylenevinylene).

Polyradical Formation and Its Electrochemistry. *p*-, *m*-, and *o*-**2** were obtained by heterogeneously treating the benzene solutions of *p*-, *m*-, and *o*-**2′** with fresh PbO_2 powder or aqueous alkaline $K_3Fe(CN)_6$ solution, respectively (Scheme 1), and isolated as brown-green powders. The polyradicals were also soluble in common solvents. GPC elution curves of the polymers before and after the radical generation (*i.e.*, **2′** and **2**) coincided with each other. This is consistent with the assumption that the oxidation does not bring about oxidative degradation or cross-linking of the main chain.

The polyradical was also generated by electrochemical oxidation (Scheme 2, FC = a ferromagnetic coupler). The *m*-phenylene-linked diphenolate anion of **6′** [22] displays two reversible redox waves in cyclic voltammetry and differential pulse voltammetry (Figure 1a; for details see the supporting information), which correspond to the formation of the radical anion and the diradical. On the other hand, the stilbene-linked diphenolate anion derivative of *o*-**4′** gave reversible but simple cyclic and differential pulse voltammograms (Figure 1b): The redox potential and the half-current width in the differential pulse voltammetry agreed with those of the monomeric phenolate derivative of *o*-**3′** and of 2,4,6-tri-*tert*-butylphenol (as the

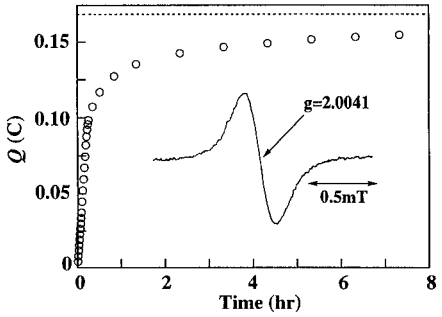

Figure 2. Controlled potential coulometric oxidation of the polyphenolate anion of *o*-**2′** and electrolytic ESR spectrum for *o*-**2′**.

controls for a simple one-electron transfer reaction) under the same conditions.

Coulometric oxidation of the poly(phenolate anion) of *o*-**2′** on a large-area platinum gauze electrode indicated almost stoichiometric oxidation (Figure 2). The total number of electrons transferred per polymer molecule is very close to the DP of the polymer. Electrolytic ESR spectroscopy (example given in the inset in Figure 2) supported the formation of the phenoxyl radicals. Under the same conditions, *o*-**2′** also gave a reversible but isopotential cyclic and differential pulse voltammogram like that of *o*-**4′** (Figure 1c). The successive electron transfers along the polymer skeleton follow the simple statistics of noninteracting groups, as has been discussed for poly(vinylferrocene).[23] The π-conjugated and alternant but non-Kekulé-type structures of **6′**, *o*-**4′**, and *o*-**2′** exclude a quinoid formation or two-electron transfer reaction and realize the one-electron transfer reaction represented in Scheme 2. The electrochemical study in Figures 1 and 2 brings about the following discussion. The *m*-phenylene ring in **6′** is an effective coupler between the plural organic redox sites, the phenolate anions/phenoxyl radicals, to transmit the resonance effect from each other through the π-conjugation. However, the stilbene coupler in *o*-**4′** including the poly(*o*-phenylenevinylene) skeleton in *o*-**2′** is too long in the π-conjugation and/or steric distance to induce an effect in the electron transfer reaction in Scheme 2, although the stilbene and poly(*o*-phenylenevinylene) skeletons are effective (at low temperature) as a magnetic coupler which transmits spin polarizaton between the attached plural phenoxyl radicals (mentioned below).

The cyclic voltammogram of the poly(phenolate anion)/poly(phenoxyl radical) was obtained in repeated potential sweeps. This result means that the polyradical is chemically stable even in a solution at room temperature, and that radical generation is not accompanied by a subsequent chemical side reaction.

ESR Spectra of the Polyradicals. The formation of the polyradical was supported by the appearance of the ESR signal and a new visible absorption at 700 nm attributed to the phenoxyl radical. Spin concentration was determined both by carefully integrating the ESR signal in comparison with that of the TEMPO solution as a standard and by analyzing the saturated magnetization at 2 K using a SQUID magnetometer. The spin concentration (spin concn) of **2** reached *ca.* 4.2×10^{23} spin/mol of monomer units (0.7 spin/monomer unit) under oxidizing conditions. *p*-, *m*-, and *o*-**2** were appropriately stable for maintaining the initial spin concn under the ESR and SQUID measurement conditions, and the half-life of the polyradicals was 3−5 h at room temperature in solution and *ca.* 1.5 days as powders, respectively. This long-term chemical stability of **2** is in contrast to those of previously reported cross-conjugated polyradicals:[7−9] The latter were formed only at extremely low

(21) Kossmehl, G. A. In *Handbook of Conducting Polymers*; Skotheim, T. A., Ed.; Marcel Dekker, Inc.: Basel, 1989; Vol. 1, p 351.
(22) Mukai, K.; Hara, T; Ishizu, K. *Bull. Chem. Soc. Jpn.* **1979**, *52*, 1853.
(23) Flanagan, J. B.; Margel, S., Bard, A. J.; Anson, F. C. *J. Am. Chem. Soc.* **1978**, *100*, 4248.

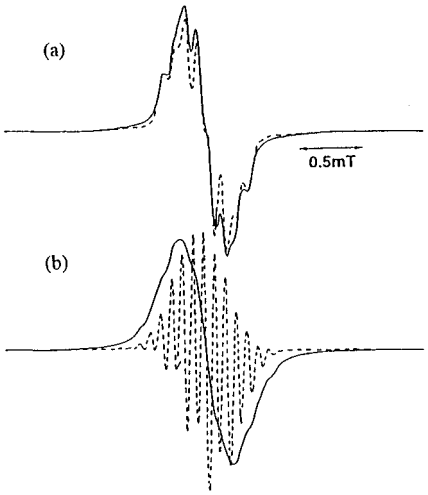

Figure 3. ESR spectra of the radicals at room temperature. (a) the solid line for *p*-**2** in benzene at $g = 2.0045$, polymer concn = 0.5 unit mM (spin concn = 0.06 spin/unit) and the dashed line for the monomeric radical *p*-**3** at $g = 2.0045$; (b) the solid line for *o*-**2** in benzene at $g = 2.0043$, polymer concn = 0.5 unit mM (spin concn = 0.04 spin/unit) and the dashed line for the monomeric radical *o*-**3** at $g = 2.0041$.

temperature and could not be isolated, except the oligo-[(oxyimino)-*m*-phenylene)s[10a] and the polychloro-substituted triphenylmethine derivatives.[10c]

The ESR spectrum of **2** at low spin concn gave a broad hyperfine structure at $g = 2.0043-2.0045$ due to unresolved coupling of the 5−7 protons of the phenoxyl ring and the phenylenevinylene skeleton (Figure 3). This is in contrast to the three-line hyperfine structure of 2,4,6-tri-*tert*-butylphenoxyl ascribed to an unpaired electron localized in the phenoxyl ring. The spin density distribution over the 4-phenyl group in *p*- and *o*-**2** was further supported by the clearer hyperfine structure of the corresponding monomeric radicals 2,6-di-*tert*-butyl-4-(4-bromo-2-vinylphenyl)phenoxyl (*p*-**3**) and 2,6-di-*tert*-butyl-4-(3-bromo-4-vinylphenyl)phenoxyl (*o*-**3**) (the dashed lines in Figure 3), whose coupling constants were estimated by spectral simulation. The ESR hyperfine coupling constants (mT) were estimated as follows: for *p*-**3**, phenyl ring substituted with phenoxyl, *o*, $a_H = 0.11$; *m*, $a_H = 0.06$; *p*, $a_H = 0.11$; vinyl, $a_H = 0.03$; phenoxyl, $a_H = 0.17$; for *o*-**3**, phenyl ring substituted with phenoxyl, *o*, $a_H = 0.17$; *m*, $a_H = 0.10$; vinyl, $a_H = 0.09$; phenoxyl, $a_H = 0.18$. These data agreed well with previously reported coupling constants for the phenoxyl radical with a similar phenyl−phenyl bond and torsional structure: 2,6-Di-*tert*-butyl-4-phenylphenoxyl without any substituent at the *o*-position of the 4-phenyl group gives a much larger proton hyperfine coupling constant attributed to the 4-phenyl group than is found in 2,6-di-*tert*-butyl-4-(2-methylphenyl)phenoxyl.[24] *o*-**2** probably also involves an effectively delocalized spin density distribution into the phenylenevinylene skeleton because of its less hindered steric structure.

The ESR spectra of *p*- and *o*-**2** showed sharp and unimodal signals with increasing spin concn, as shown in Figure 2 (inset), indicating a locally high spin concn along the polymer skeleton. A frozen toluene glass of *o*-**2** gave only a broad spectrum at $g = 2$, which could not be analyzed because of the presence of several conformers and the long distance between unpaired electrons in the polyradical. The frozen toluene glass of a 10 mM *o*-**2** with a spin concn of *ca.* 0.5 spin/unit gave a $\Delta M_s = \pm 2$ forbidden transition ascribed to a triplet species at $g = 4$ (inset in Figure 4). The ESR signals in the $\Delta M_s = \pm 2$ region

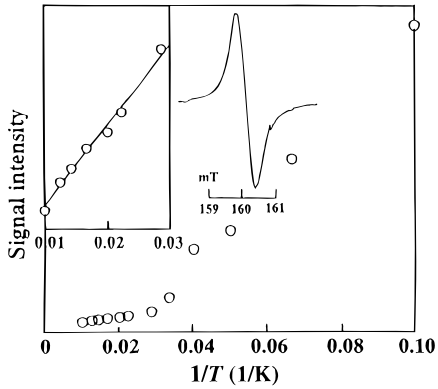

Figure 4. Curie plots for the peak in the $\Delta M_s = \pm 2$ region for the polyradical *o*-**2** with spin concn = 0.5 spin/unit in toluene glass (inset, $\Delta M_s = \pm 2$ spectrum).

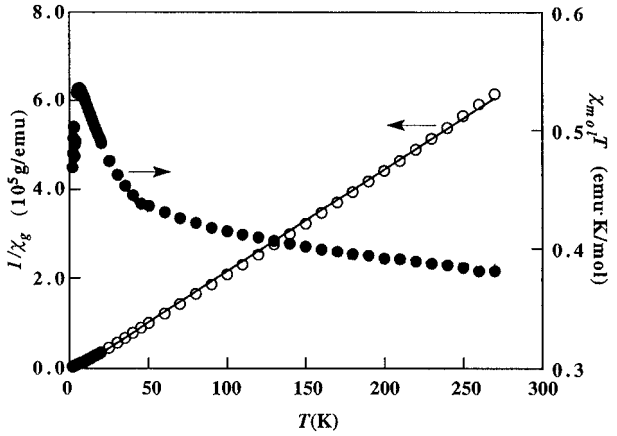

Figure 5. $1/\chi_g$ *vs T* plots (○) with the Curie−Weiss fitting (solid line) and $\chi_{mol}T$ *vs T* plots (●) of the powder sample of *p*-**2** with spin concn = 0.36 spin/unit.

were doubly integrated by varying the temperature to give Curie plots (Figure 4). Although the signal intensity is essentially proportional to the reciprocal of the absolute temperature ($1/T$) at higher temperature, the plots substantially deviate upward from linearity in the lower temperature region. This upward deviation suggests a ferromagnetic interaction between the triplet species in the polyradical *o*-**2**.

Magnetic Properties. Static magnetic susceptibility and magnetization of **2** were measured with a SQUID magnetometer. The gram magnetic susceptibility (χ_g) of the polyradicals in the powder sample followed the Curie−Weiss law ($\chi_g = C/(T - \theta_w)$),[25] as shown in Figure 5 using the example of *p*-**2**. The Curie−Weiss behavior was reversible during temperature depression and elevation, which indicates chemical stability of the polyradical. The Curie constant (C) and Weiss temperature (θ_w) were estimated by linear fitting to $1/\chi_g$ *vs T* plots, giving, *e.g.*, 4.4×10^{-4} (emu·K)/g and 5.7 K at 10−280 K for *p*-**2**. The spin concn estimated from the Curie constant was 0.36 spin/unit, and agreed both with those from integration of the ESR signal compared with that of a TEMPO (2,2,6,6-tetramethyl-1-piperidinyloxyl) solution, and with saturated magnetization at 2 K using a SQUID magnetometer. The plots of the product of molar magnetic susceptibility (χ_{mol}) and T *vs T* are also shown in Figure 5. $\chi_{mol}T$ increases at low temperature (50−200 K) from the theoretical value for $S = 1/2$ ($\chi_{mol}T = 0.375$ (emu·K)/mol), suggesting a ferromagnetic interaction. However, the plots enormously decrease at low temperature (<20 K), indicating a strong antiferromagnetic interaction under these conditions.

(24) Icli, S.; Kreilick, R. W. *J. Phys. Chem.* **1971**, *75*, 3462.

(25) Carlin, R. L. *Magneto Chemistry*; Springer-Verlag: Berlin, 1986.

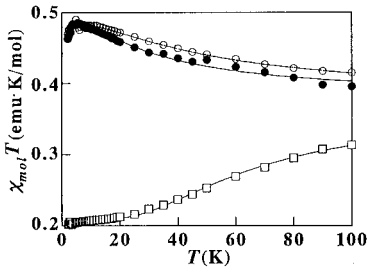

Figure 6. $\chi_{mol}T$ *vs* T plots (●) of *p*-**2** with spin concn = 0.23 spin/unit, (○) of *o*-**2** with spin concn = 0.26 spin/unit, and (□) of *m*-**2** with spin concn = 0.35 spin/unit in frozen 2-methyltetrahydrofuran. Solid lines are theoretical curves calculated using eq 5 for *p*-**2** ($2\bar{J}$ = 31 cm^{-1}, θ = −0.14 K, x_1 = 0.40, x_2 = 0.24, x_3 = 0.36), for *o*-**2** ($2\bar{J}$ = 50 cm^{-1}, θ = −0.05 K, x_1 = 0.43, x_2 = 0.25, x_3 = 0.32), and for *m*-**2** ($2\bar{J}$ = −86 cm^{-1}, θ = −0.11 K, x_1 = 0.56, x_2 = 0.44, x_3 = 0.00).

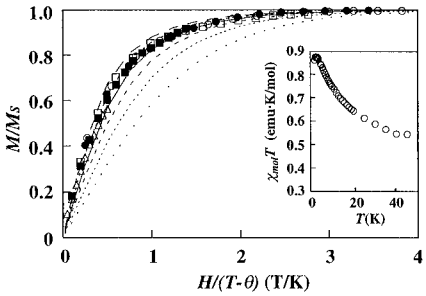

Figure 7. Normalized plots of magnetization (M/M_s) *vs* the ratio of magnetic field and temperature ($H/(T-\theta)$) for the polyradical *o*-**2** with (DP = 17) and spin concn = 0.68 spin/unit in frozen 2-methyltetrahydrofuran at T = 1.8 (○), 2 (●), 2.5 (□), 5 (■), 10 (△) K and the theoretical curves corresponding to the S = 1/2, 1, 3/2, 2, 5/2, and 3 Brillouin functions, where θ is a weak antiferromagnetic term and was determined to be −0.1 K from the $\chi_{mol}T$ *vs* T plots. Inset: $\chi_{mol}T$ *vs* T plots for *o*-**2**.

The polyradicals **2** were diluted in diamagnetic 2-methyltetrahydrofuran or toluene to minimize any antiferromagnetic and probably intermolecular interactions. The $\chi_{mol}T$ *vs* T plots for the solution sample of *p*-**2** in Figure 6 indicate a strong reduction of the antiferromagnetic interaction observed in the powder sample at low temperature. Upward deviations of $\chi_{mol}T$ from the theoretical value for S = 1/2 in the high-temperature region are clearly observed for *p*- and *o*-**2**.

On the other hand, the $\chi_{mol}T$ curve for *m*-**2**, even for its solution sample, deviates significantly downward from the value of S = 1/2 at lower temperature, indicating a singlet GS for *m*-**2**. This result not only agrees with the theoretical prediction mentioned in the Introduction and in Table 1 but also strongly supports the validity of the experimental and analytical procedures in this paper.

The magnetization (M) normalized by saturated magnetization (M_s), M/M_s, is known to be represented by a Brillouin function. The M/M_s of *o*-**2** with DP = 17 and spin concn = 0.68 spin/unit is plotted *vs* the effective temperature ($T-\theta$), and compared with the Brillouin curves (Figure 7). θ is a coefficient of the weak (antiferro)magnetic interaction between radicals, corresponding to the Weiss temperature of the Curie−Weiss law, and is determined from curve fitting using the following $\chi_{mol}T$ *vs* T data. The M/M_s plots lie almost on the theoretical Brillouin curve for S = 5/2 at 2−5 K, indicating ferromagnetic coupling, on the average, between five unpaired electrons. The average S = 5/2 of *o*-**2** with spin concn = 0.68 spin/unit means that a defect in the radical generation is not fatal for a partial but ferromagnetic spin alignment between the pendant phenoxyl radical electrons through the π-conjugated poly(phenylenevinylene) skeleton.

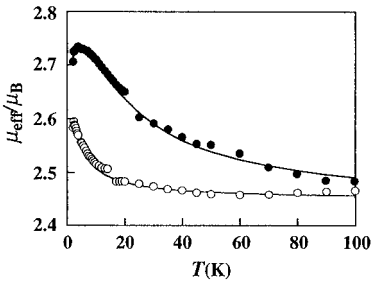

Figure 8. μ_{eff}/μ_B *vs* T plots of the diradicals *p*-**4** (●) and *p*-**5** (○). Solid lines are theoretical curves calculated using eq 4 for *p*-**4** ($2J$ = 17 cm^{-1}, θ = −0.04 K, and x_1 = 0.20) and for *p*-**5** ($2J$ = 4 cm^{-1}, θ = 0.00 K, and x_1 = 0.77).

Estimation of the Exchange Coupling Constant of the Di- and Polyradicals. The magnetization and magnetic susceptibility of the diradicals *p*-**4**, *o*-**4**, *p*-**5**, and *o*-**5** were measured in order to estimate the intramolecular spin coupling in the polyradicals **2**; **4** and **5** are the model compounds that determine the spin coupling between the neighboring units and the next neighboring units, respectively. 2-Methyltetrahydrofuran and toluene were used as a dilutent of the diradicals to minimize intermolecular interactions. The M/M_s plots of *p*-**4**, *o*-**4**, *p*-**5**, and *o*-**5** were presented close to the Brillouin curve for S = 2/2 at 2−10 K, indicating a triplet GS of the diradicals.

The ratio μ_{eff}/μ_B was calculated from eq 3,[25] where μ_{eff}, μ_B, k, χ, and N_u are the effective magnetic moment, the Bohr magneton, the Boltzmann constant, the magnetic susceptibility, and the average measured molecular number. The μ_{eff}/μ_B values

$$\mu_{eff}/\mu_B = (3k\chi TN_u)^{1/2}/\mu_B \quad (3)$$

were reduced by the spin concn determined by the ESR signal integration and by the saturated magnetization at 2 K, similar to the polyradicals, and plots of μ_{eff}/μ_B *vs* T for *p*-**4** and *p*-**5** are shown in Figure 8. The plots locate at the intermediate between μ_{eff}/μ_B = 2.45 and 2.83 for S = 1/2 and 1, respectively.

The Bleaney−Bowers expression[26] is well-known for the analysis of χ in diradicals. However, the χ of incomplete spin generation samples such as the diradicals in this study would be expressed by the sum of the complete diradical fraction and the doublet monoradical fraction.[6] The modified expression is

$$\mu_{eff}/\mu_B = \left(\frac{6g^2T}{(T-\theta)(3+\exp(-2J/kT))}(1-x_1) + \frac{3g^2T}{2(T-\theta)}x_1\right)^{1/2} \quad (4)$$

where J, θ, and x_1 are the spin-exhange coupling constant which is positive for ferromagnetic coupling, the Weiss constant for a weak intermolecular magnetic interaction, and the fraction of the doublet or monoradical species in the total spin number, respectively. Curve fitting of the μ_{eff}/μ_B data for *o*-**4** and *o*-**5** in Figure 8 to eq 4 yielded the $2J$, θ, and x_1 values given in the caption of Figure 8. The exchange coupling constant or a triplet−singlet energy gap $2J$ of the diradicals determined with eq 4 are listed in Table 2.

The positive $2J$ value of the diradicals indicates a through-bond or intramolecular ferromagnetic spin-exchange coupling in the diradicals *p*-**4**, *o*-**4**, *p*-**5**, and *o*-**5**. $2J$ is reduced to 1/5 to 1/8 (from **4** to **5**) in response to the conjugated but spacing phenylenevinylene unit. The $2J$ value of the *o*-derivatives of the diradical are larger than those of the *p*-derivatives, which

(26) Bleaney, B.; Bowers, K. D. *Proc. R. Soc. London* **1952**, *A214*, 451.

Table 2. Exchange Coupling Constants of the Polyradicals and the Diradicals

di- and polyradical[a] (DP[b])	S[c]	$2J$ or $2\bar{J}$[d] cm^{-1}
p-**4**	2/2	18 ± 1
o-**4**	2/2	50 ± 6
p-**5**	2/2	4 ± 6
o-**5**	2/2	6 ± 1
p-**2** (21)	2/2 to 3/2	32 ± 2
o-**2** (8)	1/2 to 2/2	48 ± 6
o-**2** (17)	2/2 to 3/2	47 ± 6
m-**2** (8)	0 to 1/2	−90 ± 4

[a] Spin concn for the polyradicals 0.2−0.4 spin/unit. [b] Average degree of polymerization of the precursor polymers **2′**. [c] GS S for **4** and **5** and the average spin quantum number for the spin state of **2** at 2−5 K. [d] Exchange coupling constant ($2J$) for **4** and **5** and its average value ($2\bar{J}$) for **2**.

coincides with the stronger spin density distribution for *o*-**3** in comparison with *p*-**3** estimated from the ESR hyperfine coupling constants.

The polyradical involves the contribution of various arrangements of the radical sites along the skeleton and has some spin exchange coupling constants. The spin exchange coupling constant in the polyradical was approximately estimated in this paper as the average value ($\bar{J}$) under the assumption of the exchange coupling between the neighboring units along the skeleton. We selected the polyradical samples with the spin concn of 0.2 to 0.4 spin/unit whose average GS spin quantum number was $S < 3/2$ in the M/M_s *vs* $(T - \theta)$ plots. As a first approximation, these samples with $S < 3/2$ could be expressed as the mixture of a three-, two-, and one-spin system, and we could apply the following van Vleck expression[27] to analyze the $\chi_{mol}T$:

$$\chi_{mol}T = \frac{N_A g^2 \mu_B{}^2 T}{k(T-\theta)}\left(\frac{x_3}{12}\frac{1+\exp(-2\bar{J}/kT)+10\exp(\bar{J}/kT)}{1+\exp(-2\bar{J}/kT)+2\exp(\bar{J}/kT)} + \frac{x_2}{3+\exp(-2\bar{J}/kT)} + \frac{x_1}{4}\right) \quad (5)$$

where $\bar{J}$, x_1, x_2, and x_3 are the average value of the exchange coupling constants and the fractions of the doublet, the triplet, and the quartet, respectively. The average $2\bar{J}$ was estimated from curve fitting of the $\chi_{mol}T$ *vs* T data to eq 5 (the solid lines in Figure 6), and also given in Table 2. The $2\bar{J}$ values of the polyradicals are larger than the $2J$ of the corresponding diradicals. This polymer effect is consistent with our calculation[16] and probably could be explained as follows: the spin exchange interaction cooperatively works from both sides along the conjugated skeleton, and/or the high-spin state of the polyradical is stabilized by more degenerated NBMOs due to its developed π-conjugation indicated by the UV−vis absorption maxima and I^{th} (described in the Characterization section). Comparison of *p*-**2** and *o*-**2** reveals a stronger interaction in *o*-**2**, in which the above-mentioned ESR result suggested a more effective spin distribution through the pendant phenoxyl to the backbone conjugation presumably due to its coplanarity in the π-conjugation.

Estimation of a Stiff Skeleton from the Instrinsic Viscosity. In order to estimate a stiff shape of the poly(phenylenevinylene) derivatives in this study, the dilute solution viscosity of the polymer was measured for *p*-**2′** in chloroform at 25 °C. The plot of logarithmic intrinsic viscosity ($[\eta]$) *vs* logarithmic molecular weight (M) of the polymer obeys the classical Mark-Houwink relationship[28]

$$[\eta] = KM^{\alpha} \quad (6)$$

to give the constants K (=4.9 × 10^{-3} mL/g) and α (=1.2). The α value exceeds the range $0.5 < \alpha < 0.8$ for flexible polymers,[28] which suggests a rodlike or stiff-chain conformation for *p*-**2′** (refer, *e.g.*, to α = *ca.* 0.7 and 1.1 for polystyrene in benzene[29] and poly(*p*-phenylene terephthalamide) Kevlar in concn sulfuric acid,[30] respectively).

Computational Studies of Conformational Preferences. It is not straightforward to decide what conformer predominates in the poly(1,2-, 1,5-, and 1,4-phenylenevinylene) backbones. UV−vis and IR spectroscopies can give some information, but are seldom definitive. Computational chemistry is appropriate to try to rule out conformers that are energetically disfavorable, as long as there is a considerable preference for one conformer over another. We, therefore, carried out force field calculations on polymers *o*-**2′**, *m*-**2′**, and *p*-**2′** (Scheme 1) to determine which conformers were energetically most likely. The calculations were carried out using the UFF force field, which we have found to give reasonably good bond lengths and relative steric energies for polyconjugated molecules. We assumed that all 1,2-ethenediyl groups have the *trans*- or *E*-configuration, in accord with the typical preference of the Heck reaction methodology used to synthesize these polymers. Full geometry optimization was carried out on the unoxidized polymer forms **2′**, since dependable force field parameters are not available for the polyradicals themselves. It is, therefore, worth noting at the outset that the polyradicals themselves may contain structural defects that alter local conformational tendencies relative to the unoxidized precursors. However, we feel that steric tendencies are likely to control the conformational preferences of both the polyphenols and the polyradicals.

In the *p*-polymer-based *p*-**2′**, the natural geometry of *all-trans* poly(phenylenevinylene) requires a linear, rodlike backbone. Due to possible rotation of the 1,4-phenylene groups, any neighboring pair of pendant phenoxyl groups may be either *syn* or *anti* to one another. Our computations focused on some all-alternating *anti*-conformers, and the *all-syn*-conformer, shown in Figure 9. Interestingly, the *all-syn*-conformer is found to be more stable than the all-alternating conformers by *ca.* 5 kcal/mol of monomer units. The source of strain in the all-alternating conformers appears to be the proximity of the pendant phenoxyl groups to the ethylenic C−H bonds. For the alternant conformers, the pendant group is forced into one C−H bond by the rigid poly(phenylenevinylene) backbone, as shown in Figure 9. This does not occur for the *all-syn*-conformer, which is thus preferred by a considerable margin. There is no experimental evidence which unequivocally supports this prediction, but the size of the preference in the calculation argues in favor of an *all-syn-p*-**2**. AM1-CI computations on model diradicals for *p*-**2** show a preference for the triplet state by *ca.* 200 cm^{-1} for both conformers.

The *m*-polymer *m*-**2′** may form either extended or helical conformations, shown in Figure 10. There are two types of extended conformers, which we refer to as the sinusoidal and linear conformers in Figure 10. The difference between the two extended conformers lies in the relative conformation of the ethylenic group relative to the pendant group. For the

(27) Vleck, J. H. V. *The Theory of Electric and Magnetic Susceptibilities*; Oxford University Press: London, 1932.

(28) Morawetz, H. *Macromolecules in Solution*; Interscience: New York, 1975; pp 324−335.

(29) Brandrup, J.; Immergut, E. H. *Polymer Handbook*, 3rd ed.; John Wiley: New York, 1989; Chapter VII.

(30) Foo, C.; MacBeen,J.; Xu, Z.; Okamoto, Y. *Polym. Adv. Technol.* **1993**, *4*, 106.

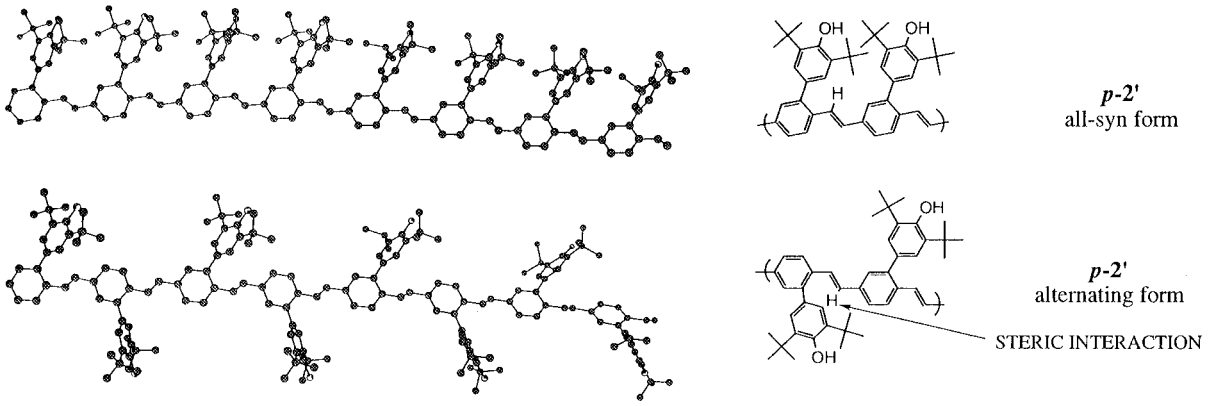

Figure 9. Optimized structure diagrams of the *p*-polymer *p*-**2′**.

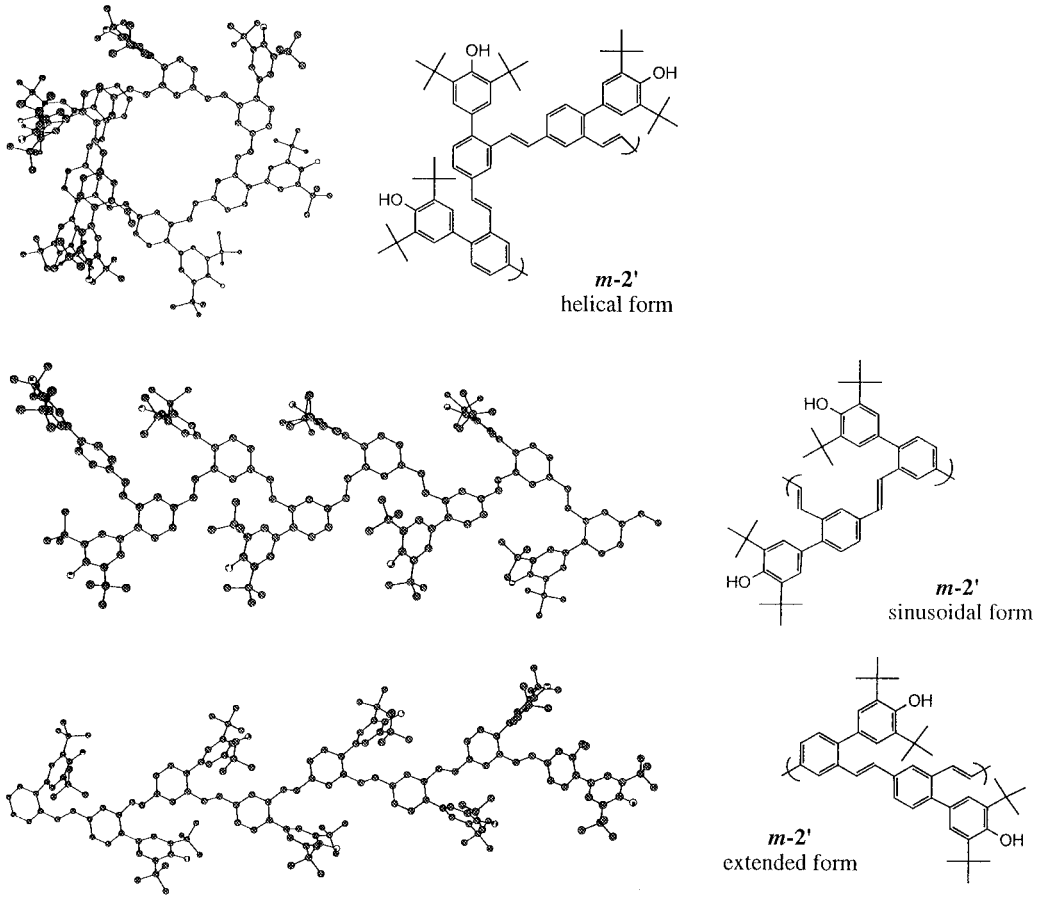

Figure 10. Optimized structure diagrams of the *m*-polymer *m*-**2′**.

sinusoidal conformer, the ethylenic groups point away from the pendant group, while in the linear conformer, the ethylenic groups point parallel to the pendant group. The helical conformer has ethylenic groups with alternating geometry relative to the pendant group, leading to the loose helix shown in the figure. Overall, the nonplanar helical form is the most stable by *ca.* 5 kcal/mol of monomer units by comparison to both extended conformers, which have nearly the same steric energy. A breakdown of the steric energy components of these conformers shows that the main source of relative instability in the planar *m*-polymer is van der Waals repulsion between the pendant groups and the *m*-backbone chain in the extended conformers. In the helical form, the pendant groups are sufficiently distant from one another to limit such interactions. Since the nonplanar conformer of *m*-**2** is a very loose helix, it seems likely that the actual conformation could twist considerably away from this idealized geometry. AM1-CI calculations on model diradicals for all the confomers of *m*-**2** show a slight favoring of the triplet state by ≤ 100 cm^{-1}. The experimental magnetic results show antiferromagnetic coupling, a result consistent with the very weak exchange computed in these cases.

The *o*-polymer *o*-**2′** has two major conformers available, a reasonably extended form and a strongly helical form as shown in Figure 11. At the UFF level of theory there is a modest preference for the planarized form, *ca*. 1 kcal/mol of monomer unit, in which the pendant phenoxyl groups are arranged in an alternating relative to the backbone. In the less stable form, all the phenoxyl group radiate outward from a central core helix of approximate 3,3 repeat symmetry. The computational finding that favors a planarized structure for the *o*-polyradicals is consistent with the notion that good π-conjugation favors high spin coupling in a pendant polyradical. Thus, *o*-**2** presumably shows intramacromolecular ferromagnetic coupling because it can assume the planarized conformation in a substantial number

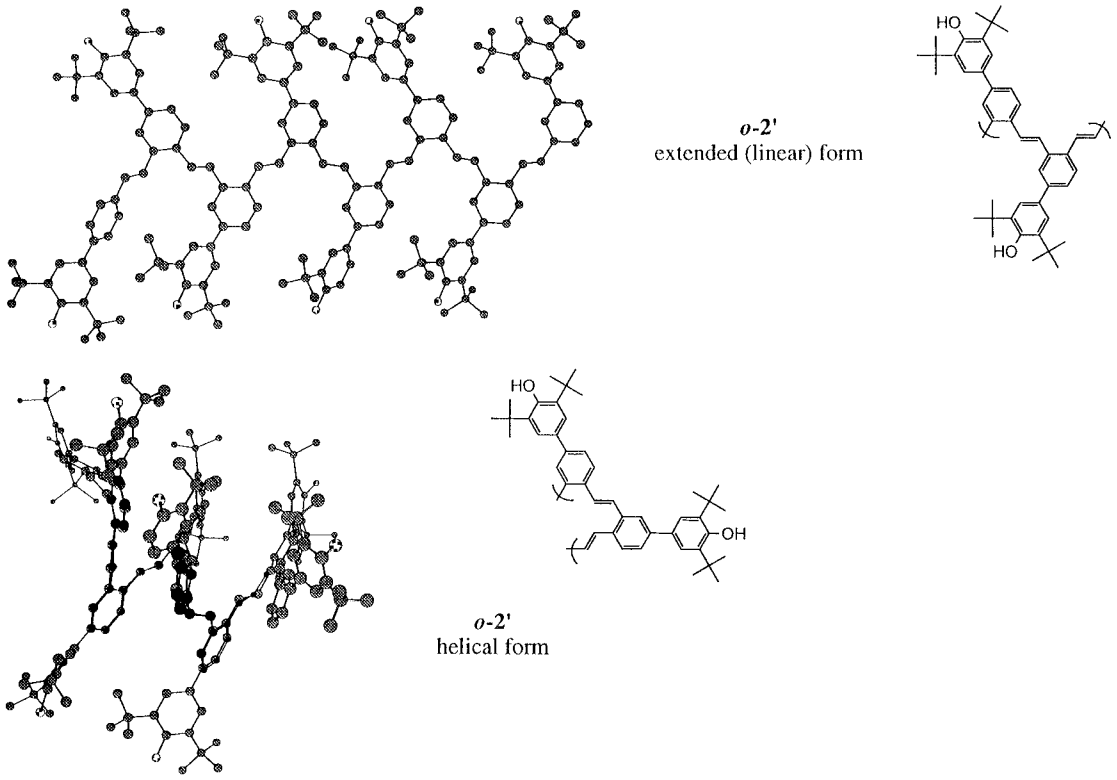

Figure 11. Optimized structure diagrams of the *o*-polymer *o*-**2′**.

of the chains present in any given sample. AM1-CI computations on model diradicals for *o*-**2** show a significant preference for the triplet state by ≥ 350 cm^{-1} in both the linear and helical conformers. The computational preference for ferromagnetic coupling qualitatively coincides with the experimental 2*J* value for *o*-**4** in Table 2 and supports the idea that the *o*-poly(phenylenevinylene) skeleton is a good choice for ferromagnetic coupling of pendant polyradicals.

The computations are in good agreement with the experimental results, and also are suggestive concerning which conformations are dominant in the actual materials. Some mixtures of conformations are possible, or even likely, in the experimental polymers, but the congruence of computational modeling results with the observed magnetic behavior of the π-conjugated polyradicals supports the value of the computer-aided design approach used by us. We hope that a similar approach will enable the identification of other ferromagnetically coupled pendant polyradicals.[31]

Conclusion

An intramolecular, through-bond, and long-range ferromagnetic exchange interaction was realized between the unpaired electrons of phenoxyl radicals attached to the π-conjugated poly(phenylenevinylene) skeleton, in accordance with the theoretical prediction based on the molecular connectivity. Average values of the exchange coupling constant for the polyradicals were larger than the exchange coupling constants for the diradicals, which suggested a cooperativity in the interaction between the multielectrons attached along the π-conjugated skeleton. The strongest ferromagnetic behavior was observed for the *o*-polyradical (*o*-**2**) which has a higher molecular weight and less hindered steric structure or more planarized π-conjugation. The *o*-**2** with spin concn = 0.68 revealed an average *S* value of 5/2, which is expected to be very enhanced with the spin concentration.

(31) Yoshizawa, K.; Hoffmann, R. *J. Am. Chem. Soc.* **1995**, *117*, 6921.

Experimental Section

Synthetic Procedures. 2-Bromo-4-(3,5-di-*tert*-butyl-4-acetoxyphenyl)styrene (*o*-3′′). *N*-Bromosuccinimide (8.8 g, 50 mmol) and benzyl peroxide (0.1 g, 0.5 mmol) were suspended in the carbon tetrachloride solution (90 mL) of 2-bromo-4-(3,5-di-*tert*-butyl-4-acetoxyphenyl)toluene (21 g, 50 mmol), and refluxed until succinimide floated on the solution. The mixture was cooled to room temperature and filtered off. After the filtrate was evaporated, benzene (100 mL) and triphenylphosphine (13 g, 50 mmol) were added to it. The resulting solution was stirred at 50 °C for 2 h. After evaporation, excess reactants were removed by chromatography on silica gel with hexane/chloroform (1/1) as an eluent, and the residue was eluted with methanol and evaporated to give the phosphonium salt (27 g): yield 71%.

The phosphonium salt (27 g, 35 mmol) was suspended in 25% formaldehyde (230 mL), and 5 N NaOH (53 mL) was added dropwise over 20 min at room temperature. The mixture was stirred for 1 h and extracted with ether. The extract was washed with water, dried over anhydrous sodium sulfate, and then evaporated. The crude product was purified by silica gel column separation with hexane elution. It was recrystallized from hexane to give rhombic or needle crystals of 2-bromo-4-(3,5-di-*tert*-butyl-4-acetoxyphenyl)styrene (*o*-**3′′**): yield 35%; mp 90 °C; IR (KBr, cm^{-1}) 1763 ($\nu_{C=O}$), 1626 ($\nu_{C=C}$); ^{1}H-NMR ($CDCl_3$, 270 MHz, ppm): δ 1.39 (s, 18H, *tert*-butyl), 2.37 (s, 3H, $-$OC(O)-CH_3), 5.38 (d, 1H, 11 Hz, $-$CH=C**H**$_2$), 5.74 (d, 1H, 17 Hz, $-$CH=C**H**$_2$), 7.09 (dd, 1H, 11 Hz, 17 Hz, $-$C**H**=CH$_2$), 7.45$-$7.48 (m, 3H, phenyl), 7.60 (d, 1H, 8 Hz, phenyl), 7.73 (d, 1H, 2 Hz, phenyl); ^{13}C-NMR ($CDCl_3$, ppm): δ 22.68, 31.46, 35.58, 116.53, 123.88, 125.21, 126.45, 126.83, 131.41, 135.42, 135.95, 136.39, 142.62, 142.96, 148.01, 171.07; MS (*m*/*z*) 428, 430 (M^+, $M^+ + 2$), calcd for M = 429.4. Anal. Calcd for ($C_{24}H_{29}O_2Br$): C, 67.1; H, 6.8; Br, 18.6. Found: C, 67.0; H, 6.6; Br, 18.5. Other bromostyrene derivatives were synthesized analogously.

Polymerization. Polymerization was carried out by modifying the conditions described in the literature.[18] Palladium acetate, tri-*o*-tolylphosphine, and triethylamine were added to 0.1$-$0.5 M monomer solution in DMF, and the mixture was heated at 100 °C (70 °C for *p*-**3I′′**) for 24 h. The polymerization conditions are listed in Table 3. The polymer was separated by polystyrene-gel permeation chromatography and was purified by reprecipitating twice from chloroform in methanol or methanol/benzene (7/3) to yield polymers as yellow

Table 3. Examples of the Polymerization and Molecular Weight of the Polymers[a]

		acetoxy polymers **2″**			hydroxy polymers **2′**		
monomer	$[M]_0$, M	yield, %	$\overline{M_w}/10^3$	$\overline{M_w}/\overline{M_n}$	yield, %	$\overline{M_w}/10^3$	$\overline{M_w}/\overline{M_n}$
p-**3″**	0.1	51	11.0	1.9	60[c]	11.2	1.8
p-**3I″** [b]	0.1	40	2.6	1.9	60[c]	2.8	1.6
p-**3′**	0.2				24	1.8	1.4
m-**3″**	0.5	41	4.5	1.5	60[c]	4.7	1.3
o-**3″**	0.5	41	4.8	1.4	44[c]	5.1	1.2

[a] $[Pd(OAc)_2]/[M]_0 = 1/10$, $[P(C_6H_4CH_3)_3]/[Pd(OAc)_2] = 2$, [triethylamine]/$[M]_0 = 2.5-5$. Temp = 100 °C except for *p*-**3I″**. Time = 24 h. Yield = methanol insoluble fraction. [b] Temp = 70 °C. [c] Yield after the elimination of the protecting acetoxy group.

powders. The molecular weight of the polymer was estimated by GPC (polystyrene-gel column, eluent THF, polystyrene calibration). Examples of the yield and the molecular weight are also given in Table 3.

Poly[4-(3,5-di-*tert*-butyl-4-acetoxyphenyl)-1,2-phenylenevinylene] (*o*-2″): IR (KBr, cm^{-1}) 1765 ($\nu_{C=O}$), 961 ($\delta_{HC=CH}$); ^{1}H-NMR ($CDCl_3$, 500 MHz, ppm): δ 1.35 (s, 18H, *tert*-butyl), 2.32 (s, 3H, $-OC(O)CH_3$), 7.0−8.0 (m, 7H, Ar, CH=CH); ^{13}C-NMR ($CDCl_3$, ppm): δ 22.71, 31.58, 35.62, 125.40, 125.56, 126.87, 127.22, 128.39, 130.29, 134.86, 136.67, 137.96, 141.40, 142.79, 147.72, 171.13. Anal. Calcd for $C_{24n}H_{28n+1}BrO_{2n}$ ($n = 14$): C, 81.4; H, 8.0; Br, 1.6. Found: C, 81.0; H, 8.2; Br, 1.4.

Poly[4-(3,5-di-*tert*-butyl-4-hydroxyphenyl)-1,2-phenylenevinylene] (*o*-2′). Poly[4-(3,5-di-*tert*-butyl-4-acetoxyphenyl)-1,2-phenylenevinylene] (1 g) was dissolved in a slight amount of THF. To its suspension in DMSO (200 mL) was added 2.5 N KOH (10 mL) under a nitrogen atmosphere. The solution was stirred at 40−50 °C for 12 h, cooled to room temperature, and neutralized with 1 N HCl. The organic product was extracted with chloroform, washed with water, and dried over anhydrous sodium sulfate. The chloroform layer was evaporated and poured into methanol. The IR spectrum of the polymer clearly indicated the complete disappearance of the C=O stretching bands at 1765 cm^{-1} attributed to *o*-**2″**, and the appearance of the sharp absorption at 3640 cm^{-1} ascribed to the sterically hindered phenolic hydroxy group. In the ^{1}H-NMR spectra, the peaks assigned to the acetyl group at 2.32 ppm (s, 3H, CH_3) completely disappeared: yield 44%; IR (KBr, cm^{-1}) 3642 (ν_{O-H}), 961 ($\delta_{HC=CH}$); ^{1}H-NMR ($CDCl_3$, 500 MHz, ppm) δ 1.45 (s, 18H, *tert*-butyl), 5.24 (s, 1H, OH), 7.39−7.78 (m, 7H, Ar, CH=CH); ^{13}C-NMR ($CDCl_3$, ppm) δ 30.32, 34.42, 123.76, 123.89, 125.01, 126.71, 128.11, 128.59, 132.13, 134.15, 136.27, 136.59, 141.90, 153.63. Anal. Calcd for $C_{23n}H_{26n+1}BrO_n$ ($n = 17$): C, 85.5; H, 8.1; Br, 1.4. Found: C, 85.1; H, 8.3; Br, 1.2. Other hydroxyl polymers were prepared analogously from the corresponding acetoxy polymers.

1-[2-Methyl-5-(3,5-di-*tert*-butyl-4-hydroxyphenyl)styryl]-2-[4-(3,5-di-*tert*-butyl-4-hydroxyphenyl)styryl]benzene (*o*-5′). 1-[2-Methyl-5-(3,5-di-*tert*-butyl-4-hydroxyphenyl)styryl]-2-[4-(3,5-di-*tert*-butyl-4-hydroxyphenyl)styryl]benzene was also prepared *via* the same Heck reaction with 2-bromo-4-(3,5-di-*tert*-butyl-4-acetoxyphenyl)toluene, 2-bromotoluene, and 4-(3,5-di-*tert*-butyl-4-acetoxyphenyl)styrene: yield 9%; mp 236 °C; IR (KBr pellet, cm^{-1}) 3640 (ν_{O-H}), 963 ($\delta_{HC=CH}$); ^{1}H-NMR ($CDCl_3$, 270 MHz, ppm) δ 1.46 (s, 18H, *tert*-butyl), 1.48 (s, 18H, *tert*-butyl), 2.29 (s, 3H, CH_3), 5.22 (s, 1H, OH), 5.27 (s, 1H, OH), 6.97−7.75 (m, 19H, Ph); ^{13}C-NMR ($CDCl_3$, ppm) δ 19.55, 30.26, 34.42, 123.78, 123.97, 124.20, 125.95, 126.47, 126.72, 126.93, 127.13, 127.67, 127.78, 128.03, 128.82, 129.49, 130.76, 130.94, 132.00, 132.54, 134.12, 135.56, 136.20, 136.37, 136.78, 140.48, 141.51, 153.40, 153.60; MS (*m*/*z*) 704, 705, 706 (M^+, $M^+ + 1$, $M^+ + 2$), calcd for M = 705.0. Other oligomers were synthesized analogously from the corresponding bromo(3,5-di-*tert*-butyl-4-acetoxyphenyl)toluene, bromotoluene, and (3,5-di-*tert*-butyl-4-acetoxyphenyl)styrene isomers.

Oxidation. The hydroxyl precursors were carefully oxidized with freshly prepared PbO_2 (solid powder) or (phase-separateed) aqueous alkaline $K_3Fe(CN)_6$ under an inert atmosphere to yield the corresponding diradicals and polyradicals.

Magnetic Measurement. The solution of radicals immediately after oxidation was used to give the samples diluted with diamagnetic 2-methyltetrahydrofuran. Powder samples were prepared as previously described. Each sample solution or powder was contained in a diamagnetic capsule. Magnetization and static magnetic susceptibility were measured with a Quantum Design MPMS-7 SQUID magnetometer. The magnetization was measured from 0.5 to 7 T at 2, 2.25, 2.5, 3, 5, and 10 K. The static magnetic susceptibility was measured from 2 to 300 K in a field of 0.5 T.

Computational Methods. All polymer structures were generated on a Silicon Graphics Indigo R4000 workstation using the Cerius^2 v.2.0 suite of programs from Molecular Simulations Inc. Force field optimizations were carried out using the unified force field (UFF; v.1.01) method of Goddard *et al*.[32] as part of Cerius^2. Computations of relative singlet and triplet energies were carried out using the AM1 Hamiltonian on frozen model geometries with the program MOPAC93[33] having the keyword sequence AM1 1SCF MECI OPEN(2,2) C.I.=(6,2) MS=n,[13a,34] where n = 0 for a singlet state and n = 1 for a triplet state. The model geometries were obtained using two linked monomeric units from the central portion UFF optimized octamer chain.

Acknowledgment. This work was partially supported by a Grant-in-Aid for Scientific Research (Nos. 228/04242104 and 277/08246101) from the Ministry of Education, Science and Culture, Japan. P.M.L. acknowledges financial support from the National Science Foundation (Grants CHE-920695 and -9521594). We also acknowledge special software support from Molecular Simulations Inc.

Supporting Information Available: Synthetic and analytical data of 2-bromo-4-(3,5-di-*tert*-butyl-4-acetoxyphenyl)toluene, analytical data of monomers, polymers, and oligomers other than those described in the Experimental Section, and experimental details of measurements (5 pages). See any current masthead page for ordering and Internet access instructions.

JA961721U

(32) Rappe, A. K.; Casewit, C. J.; Colwell, K. S.; Goddard, W. A., III; Skiff, W. M. *J. Am. Chem. Soc.* **1992**, *114*, 10024.
(33) Stewart, J. J. P. *QCPE, Program 455*, 1989.
(34) Ichimura, A.; Koga, N.; Iwamura, H. *J. Phys. Org. Chem.* **1994**, *7*, 207.